

Free-Space Optical Channel Turbulence Prediction: A Machine Learning Approach

Md Zobaer Islam, Ethan Abele, Fahim Ferdous Hossain, Arsalan Ahmad, *Senior Member, IEEE*,
Sabit Ekin, *Senior Member, IEEE*, and John F. O'Hara, *Senior Member, IEEE*

Abstract—Channel turbulence presents a formidable obstacle for free-space optical (FSO) communication. Anticipation of turbulence levels is highly important for mitigating disruptions. We study the application of machine learning (ML) to FSO data streams to rapidly predict channel turbulence levels with no additional sensing hardware. An optical bit stream was transmitted through a controlled channel in the lab under six distinct turbulence levels, and the efficacy of using ML to classify turbulence levels was examined. ML-based turbulence level classification was found to be $> 98\%$ accurate with multiple ML training parameters, but highly dependent upon the timescale of changes between turbulence levels.

Index Terms—Free space optical communication, channel turbulence prediction.

I. INTRODUCTION

Free-space optical (FSO) communication is emerging as a critical technology for high-speed, wireless transmission of data in certain applications. Specifically, FSO is valuable in scenarios where establishing the traditional infrastructure for guided-wave communication is either impractical or impossible. The benefits of FSO over radio frequency (RF) wireless systems are substantial: enhanced security, reduced size, weight, and power (SWaP), and increased bandwidth, particularly over very large distances (> 300 km). As such, FSO is rapidly becoming a necessity in satellite communications, lunar communication, and deep space exploration. Of course it continues to find new applications in terrestrial point-to-point links as well.

Despite its numerous advantages, FSO still faces significant practical challenges. One critical factor impeding the reliability and performance of FSO links is atmospheric turbulence [1]–[3]. Turbulence is a physical phenomenon that refers to the

random fluctuations in the refractive index of the atmosphere [4]. These fluctuations cause variations in the intensity and phase of the transmitted optical signal, leading to beam wander and scintillation effects at the receiver [5]. These effects cause signal fading, distortion, increased bit-error rates, and generally poorer performance or reduced reliability of the whole system. Furthermore, because it is produced by temperature differentials between the Earth and atmosphere [4], its severity changes as a function of both location and time.

Turbulence is a major loss factor in most FSO systems [6], [7] and link budgets must be adequately crafted to achieve robust and dependable FSO communication, particularly for links between Earth and satellites or terrestrial applications. A great deal of effort has been focused on overcoming it by various means, including selection of transmitted power, adaptive optics, and optimization of beam width [8]. However, many of these methods require or benefit from an accurate estimate of the turbulence levels, which is needed to determine the variance of the beam center, receiver power, and other important parameters. A common and important parameter used in classifying turbulence level is the refractive index structure constant C_n^2 , which changes as a function of altitude, and may vary greatly at all altitudes throughout the day [9], [10]. Orders of magnitude difference can be seen from morning to night, with large fluctuations also occurring on the scale of minutes. A number of models have been developed to predict C_n^2 , but their accuracy is limited when used outside the region in which they were derived [7]. Several measurement techniques also exist, including scintillometers, image-based techniques, and balloon sounding [11]. However, these methods also suffer some drawbacks: image-based techniques require a visible target whose distorted image can be monitored, limiting the maximum range. Balloon-based techniques may take hours to rise through the atmosphere and complete their readings. Acoustic sounding systems add significantly to the cost, power requirement, and size of the ground station installation. FSO systems would greatly benefit from methods to quickly classify local or distance-integrated turbulence levels, particularly if existing hardware could be leveraged. This information could improve the efficiency and reliability of FSO systems by enabling adjustment of power and beam parameters, possibly in real time. For hybrid RF/FSO systems, the accurate prediction of turbulence level variations may also underpin informed switching decisions between RF and FSO links used in satellite communication systems, ultimately enhancing the overall system performance and reliability.

Conventional methods for predicting or classifying turbu-

This work was supported in part by the National Aeronautics and Space Administration under Grant 80NSSC20M0214. (*Corresponding author: Ethan Abele, John F. O'Hara.*)

Md Zobaer Islam is with the Department of Radiology, University of North Carolina at Chapel Hill, Chapel Hill, North Carolina, USA, and the School of Electrical and Computer Engineering, Oklahoma State University, Oklahoma, USA (e-mail: zobaer_islam@med.unc.edu, zobaer.islam@okstate.edu)

Ethan Abele, Fahim Ferdous Hossain, and John F. O'Hara are with the School of Electrical and Computer Engineering, Oklahoma State University, Oklahoma, USA (e-mail: eabele, fferdou, oharaj@okstate.edu)

Arsalan Ahmad is with the Department of Electrical and Computer Engineering, Iowa State University, Ames, Iowa, USA (e-mail: aahmad@iastate.edu)

Sabit Ekin is with the Departments of Engineering Technology, and Electrical & Computer Engineering, Texas A&M University, College Station, Texas, USA (e-mail: sabitekin@tamu.edu)

This work has been submitted to the IEEE for possible publication. Copyright may be transferred without notice, after which this version may no longer be accessible.

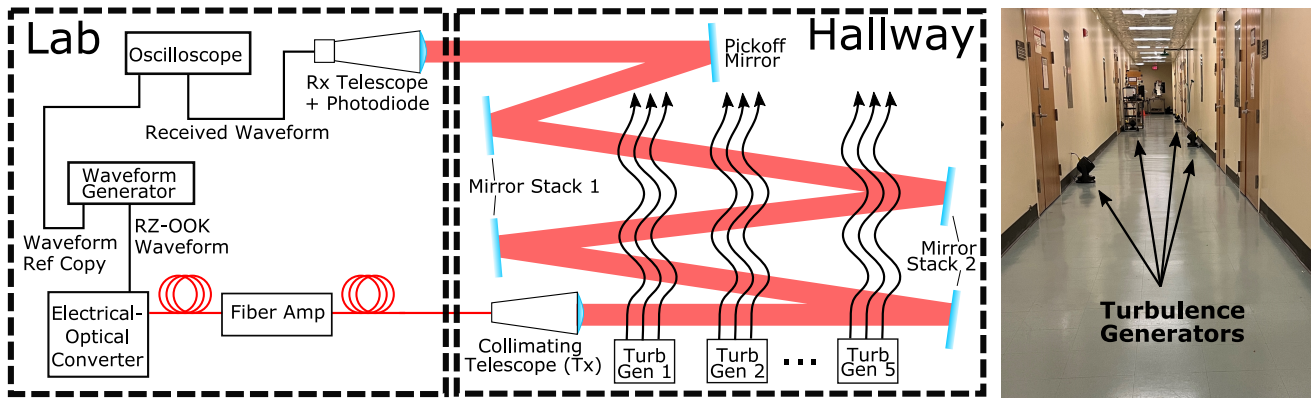


Fig. 1. System diagram showing the general connections between instruments and turbulence flow through the optical path. Part of the lab hallway is shown on the right with four turbulence generators.

lence often rely on complex mathematical models and physical simulations [12]–[14]. These approaches suffer from limitations, such as impracticality in real-time applications [15] and dynamic environments. Machine learning (ML) presents a compelling alternative for turbulence prediction in FSO channels [16], [17]. By leveraging advanced algorithms, ML enables the classification of received optical data in a more flexible and practical manner than traditional methods. The ability of ML models to discern complex patterns and relationships in data makes them well-suited for predicting turbulence and facilitating adaptive communication strategies [18]. In this study, we explore the potential of ML in turbulence prediction by providing empirical analysis of its application in classifying received optical data based on their turbulence levels in a simpler way than the other available methods in the literature. We also present some limitations of this ML method.

The rest of this paper is organized as follows. Section II describes the hardware configuration and experimental details. Section III presents the measured data and how they were collected. Section IV discusses the details of machine learning-based turbulence level prediction along with associated results. Insights drawn from the data and results are discussed in Section V. Finally, Section VI presents some conclusions from the entire effort and future directions.

II. SYSTEM DESIGN AND IMPLEMENTATION

An optical communication system with variable air turbulence has been constructed within the hallway of the Ultrafast Terahertz and Optoelectronic Laboratory (UTOL) at Oklahoma State University. The UTOL hallway, shown in Fig. 1, is well suited for testing atmospheric effects. The hallway is sealed by doors at either end, providing a relatively controlled environment in terms of temperature and airflow, along with some degree of isolation from activity in the rest of the building.

Fig. 1 illustrates the equipment setup. The transmit signal was provided by a Keysight M8195A arbitrary waveform generator (AWG) [19], which is capable of creating electrical signals with a maximum bandwidth of 25 GHz. For this work, a pseudo-random binary sequence (PRBS) was used to randomize the bit stream and avoid any bias in the results. The AWG output modulated a 1550 nm electrical-optical converter.

The optical pulses from the converter were amplified by an erbium-doped fiber amplifier and then carried by fiber optic cable to a 2-inch transmit telescope. The transmit telescope collimated the beam diverging out of the fiber. The telescope transmitted the data into the hallway path, where it reflected between mirrors at either end. The mirrors were chosen to be wider than the receiver aperture and any spatial beam fluctuations due to turbulence. This ensured that observed fading was due only to turbulence rather than beam clipping at the edge of the mirrors. The beam traversed the hallway four times in total before a final pick-off mirror directed the beam out of the hallway to a receiving telescope. The total propagation distance was approximately 172 m. The receiver (Rx) telescope collected the beam and focused it onto a photodetector. The electrical signal from the detector was captured on a Keysight DSOV254A digital storage oscilloscope (DSO) [20]. Turbulence generators were placed at regular intervals along the hallway to direct turbulent airflow across the beam path.

III. DATA COLLECTION

Utilizing the setup in Section II, optical communication data under different turbulence conditions were acquired and analyzed. The transmitted PRBS data sequence had a length of 2040 bits plus a 32 bit header so that its beginning could be easily identified in the measured data. Two repetitions of this sequence were added together and converted into return-to-zero, on-off-keying (RZ-OOK) waveforms using standard digital signal processing techniques. Both a 5 Mbps and 10 Mbps waveform were produced from this bit sequence so that multiple data rates could be tested.

The AWG was configured to output the desired waveform simultaneously on two of its output channels. One channel provided a modulation signal to the laser transmitter resulting in the OOK modulation of the emitted light. After traveling through the optical path the resulting signal at the receiving photodiode was recorded on one channel of the oscilloscope. The second AWG output was connected directly to another channel of the DSO so that an uncorrupted copy of the signal was available as ground truth (see Fig. 1). The output signal was continuously repeated so that a capture contains many thousands of bits.

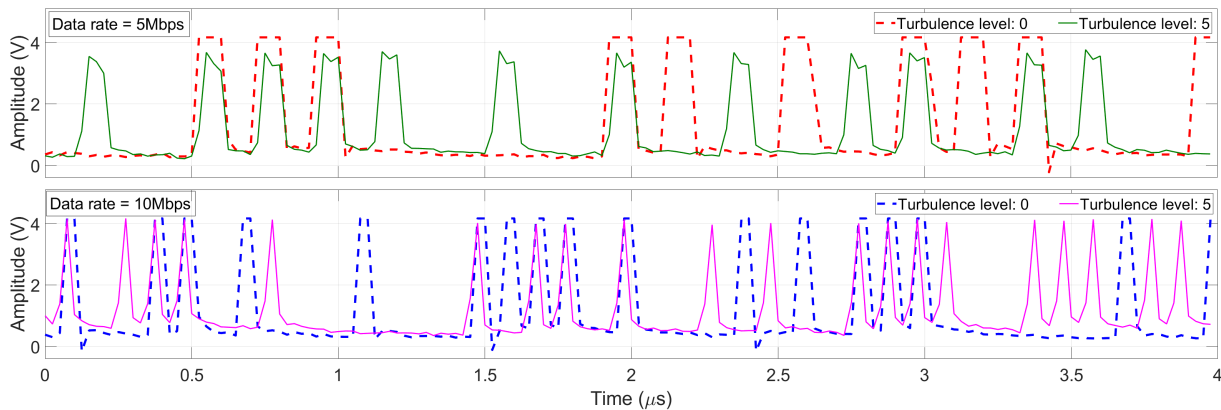


Fig. 2. Received data plots from the beginning of the first files of turbulence levels 0 and 5.

Turbulence in the test chamber was varied by changing the number of active turbulence generators in the optical path. Turbulence levels ranged from 0 to 5 fans, representing six distinct turbulence levels, with 0 denoting the least and 5 denoting the highest turbulence levels. The DSO captured the received signal for 2.5 seconds in three repetitions, generating three data files for each turbulence level. Data were collected and stored at two different rates - 5 Mbps and 10 Mbps, with 8 and 4 samples per bit, respectively. The total duration of data collection was constrained by the memory depth of the DSO. Data were captured twice following the above procedure – once immediately after activating the turbulence generators, and again after a stabilization period of 10 minutes, during which the generators operated continuously. The data were stored in .mat format and directly accessed using Python code for further processing.

Fig. 2 shows plots of first 160 samples for both data rates and for the minimum and maximum turbulence levels with zero stabilization time. Thus, it presents first 20 bits for 5 Mbps data and first 40 bits for 10 Mbps data. The graphs reveal that the bits exhibit cleaner and flatter tops for ‘1’ bits in the absence of turbulence (level 0). Conversely, at turbulence level 5, the bits exhibit partial distortion due to channel degradation resulting from higher turbulence levels. Since ‘0’ bits are represented by zero laser intensity in OOK modulation, their noise variance is unaffected by the turbulence.

IV. TURBULENCE PREDICTION

Extreme gradient boosting or XGBoost, an ensemble machine learning algorithm, was utilized to classify the received optical data based on the turbulence level. Ensemble learning methods offer enhanced classification accuracy compared to individual models, such as single decision trees, by integrating multiple models in an optimized manner. There are two primary pathways in ensemble learning: bagging and boosting [21]. Bagging techniques (e.g., random forest) take average accuracy of multiple independently-built base models. Boosting techniques excel in the bias-variance trade-off compared to bagging techniques by sequentially refining models to correct errors made by preceding ones, thereby focusing on the most informative features of the data [22]. XGBoost stands out as a popular boosting technique due to its superior power and efficiency over traditional methods like

Adaboost or gradient boosting. This superiority arises from its enhanced regularization techniques, efficient feature splitting, and parallel processing capabilities. In this study, XGBoost algorithm was implemented using the Scikit-learn library with default parameters in the Python programming language.

The class labels ranged from 0 to 5 in this study depending on the level of turbulence in the optical channel set by the turbulence generators. To gain insights into the data and devise a more effective strategy for training and predicting turbulence levels, distinct approaches were employed for selecting training and testing data. At first, three data files collected immediately after activating the turbulence generators were considered. File 2 was temporally subsequent to file 1, and file 3 was subsequent to file 2, as they were sequentially collected with an approximate 10 second time gap between consecutive files. In the initial phase, the data from the beginning of each file were independently extracted, with 1000 bits per data signal and a total data count of 4500 bits. A random 80%-20% train-test split was performed, and the turbulence classification was conducted using the XGBoost algorithm. Next, the same analysis was executed on the dataset collected after a 10 minute turbulence stabilization time. Turbulence prediction accuracies on test datasets for both cases are depicted in Table I. These accuracies indicate the success rate of the ML algorithm to predict the channel turbulence (level 0-5) categorically.

Next, another analysis using the data with zero stabilization duration was conducted. In this case, the number of bits per data instance, or equivalently the time duration considered per data, was varied to see its effect on turbulence prediction accuracy. While keeping the total number of data instances constant at 4500, the number of bits per data was varied from 200 to 3000 for all three files independently for both training and testing purposes. Again, turbulence classification was conducted with an 80%-20% train-test split. The classification accuracy scores on test data resulting from this investigation are presented in the left subplot of Fig. 3. Additionally, an examination was performed on the effect of varying the number of data instances used for training and testing on the classification accuracy. This analysis kept the number of bits per data instance constant at 1000, while varying the number of total data instances considered. The corresponding prediction accuracy scores on test data are displayed in the right subplot

TABLE I
TURBULENCE CLASSIFICATION TEST ACCURACIES (DATA COLLECTED FROM THE BEGINNING OF THE FILES, TRAIN + TEST DATA COUNT=4500, NUMBER OF BITS PER DATA=1000)

Files considered	Turbulence classification accuracy scores	
	no stabilization	10 minutes stabilization
File 1	90.00%	98.33%
File 2	98.56%	98.11%
File 3	99.11%	99.44%

of Fig. 3. To gain additional insights and comparisons, similar graphs were generated with the data collected after a 10 minute stabilization time; these are presented in Fig. 4. The ranges of x -axes in both Figs. 3 and Fig. 4 were chosen based on the convenience of segmenting data instances from the original longer-duration data files.

V. DISCUSSION

In the central column (zero stabilization time) of Table I, a discernible elevation in classification accuracy is noted as we progress temporally from file 1 to file 3. These results reveal a dynamic but converging impact of turbulence over time, leading to improved prediction accuracy. This trend is further illustrated in both subplots of Fig. 3, where classification accuracies associated with file 2 consistently surpass those linked to file 1. Moreover, the accuracies with file 3 exceed those with file 2 in the majority of cases. However, this effect is not evident in the results obtained with the data collected after 10 minutes of turbulence stabilization, as all three accuracy scores are nearly identical in the rightmost column of Table I. Furthermore, in the left subplot of Fig. 4, the accuracy scores with different files (with the same waiting period) are observed to vary randomly with all values consistently exceeding 90%. These observations substantiate the earlier inference that the turbulence effect becomes stabilized over time, yielding similar and higher prediction accuracies across all three files.

In the left subplot of Fig. 3, the increase in the number of bits per data instance introduces *greater* ambiguity in the data due to the temporal variation in the effect of turbulence, leading to a decline in turbulence prediction accuracies. However, file 3, characterized by a comparatively stabilized turbulence level, exhibits a more gradual decrease in classification accuracy compared to the other two files. When we wait to allow the turbulence to settle down, such decreasing trends are not observed, as shown in the left subplot of Fig. 4.

In the right subplots of both Figs. 3 and 4, the increase in the number of data instances, equivalent to introducing a longer time duration for the data considered for training and testing, was explored while maintaining a constant number of bits per data at 1000. As the number of data instances increases, turbulence classification accuracy initially rises for all three files, which is a common effect of increasing the number of valid data instances in most ML-based classification tasks [23]. In the right subplot of Fig. 3, the accuracies reach a peak before gradually decreasing for files 1 and 2, but the accuracy nearly saturates after the initial increase for file 3. This behavior is attributed to file 3's temporal position relative to the other two files, where the turbulence is stabilizing

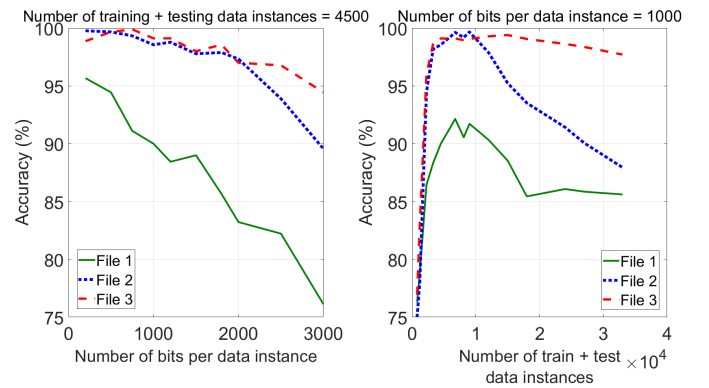


Fig. 3. Turbulence classification test accuracy scores for different files with zero stabilization time after activation of the turbulence generators (data were taken from the beginning of each file).

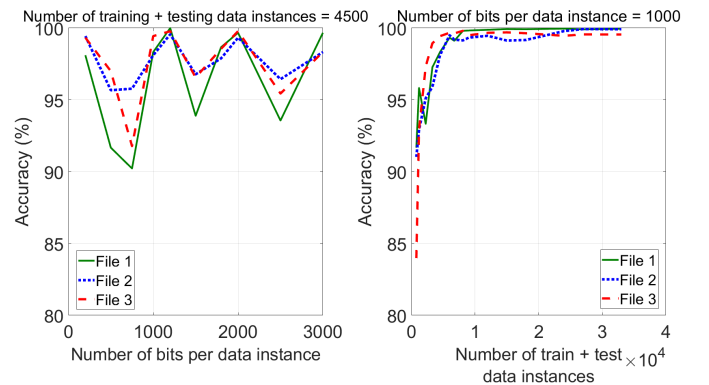


Fig. 4. Turbulence classification test accuracy scores for different files with 10 minute stabilization time after activation of the turbulence generators (data were taken from the beginning of each file).

and consideration of more data instances covering a longer time duration thereby enhances classification by accentuating the distinctions among turbulence levels. After 10 minutes, the turbulence has stabilized, therefore all three files show a similar trend in the right subplot of Fig. 4, saturating after reaching a knee point. Thus, the results presented in Figs. 3 and 4 validate the time-dependent nature of turbulence in the optical channel and its very practical effect on turbulence classification.

The results also reveal some limitations of our method. First, this method classifies discrete turbulence levels, but does not quantify C_n^2 or its variation along a path. It may be beneficial in future practice to have such data, but it is not yet clear what challenges exist in gaining that data. Second, the data reveal a time scale associated with the dynamic behavior of turbulence. During transient changes in turbulence level, ML performed more poorly, however this could be avoided by a relatively short stabilization period on the order of 1 minute or less. The atmosphere regularly exhibits both short term turbulence fluctuations (tens of minutes) and long term fluctuations from morning to evening [9], [10]. It will be important in future ML endeavors to carefully regard all such time scales and a robust ML algorithm would account for this. It is, however, promising that the algorithm's accuracy was capable of converging with only about 1 minute of stabilization. This suggests the ML method could be used for trend analysis to predict upcoming outages in real-time.

The results also suggest the ML method may enhance the performance of real world systems. Existing measurement and modeling techniques capture turbulence variations in both vertical or horizontal C_n^2 profiles. However, low earth orbit satellites transition from horizon to overhead (to some extent) and back to horizon rapidly and during every orbital pass. Therefore, the beam may traverse all possible combinations of vertical and horizontal propagation through the atmosphere, a situation for which existing techniques are far less capable. For example, it would be impractical to install sonar sounding stations with the required density to predict turbulence effects for all possible satellite links within range of a single ground station. Since the ML technique utilizes only the optical data beam, the method demonstrated here is highly economical for coarsely monitoring turbulence in a large region surrounding the ground station. This could provide a “communication weather map” built up by the ground stations themselves without need for any additional infrastructure. This could also enable additional ML techniques on a broader scale to predict FSO outages, allowing the entire communication network to react by switching to RF bands or routing data to other FSO ground stations. These are the subjects of future investigations.

VI. CONCLUSION

In conclusion, this research presented an empirically-validated, novel approach for predicting discrete turbulence levels of an optical data channel utilizing machine learning, specifically the XGBoost model. The method consistently achieved an accuracy of $> 98\%$ so long as the dynamic changes in turbulence were allowed to stabilize over about 1 minute. A temporal analysis revealed that prediction accuracy could actually degrade with more training data during turbulence stabilization periods. The study also provides valuable insights into optimizing training strategies by examining the impact of the number of bits per data instance and the number of data instances on prediction accuracy. Looking ahead, future research directions include exploring machine learning models that better adapt to real-time dynamics of atmospheric turbulence and perhaps provide more quantitative data about the channel. Tradeoff studies considering the hardware constraints for practical ML deployment may also be compared to existing methodologies. By bridging the gap between machine learning and FSO communication, this research contributes to the development of more resilient and efficient communication systems.

REFERENCES

- [1] M. Sahu, K. V. Kiran, and S. K. Das, “FSO link performance analysis with different modulation techniques under atmospheric turbulence,” in *2018 Second International Conference on Electronics, Communication and Aerospace Technology (ICECA)*. IEEE, 2018, pp. 619–623.
- [2] P. Kaur, V. K. Jain, and S. Kar, “Performance analysis of FSO array receivers in presence of atmospheric turbulence,” *IEEE Photonics Technology Letters*, vol. 26, no. 12, pp. 1165–1168, 2014.
- [3] K. Prabu, D. S. Kumar, and T. Srinivas, “Performance analysis of FSO links under strong atmospheric turbulence conditions using various modulation schemes,” *Optik*, vol. 125, no. 19, pp. 5573–5581, 2014.
- [4] L. C. Andrews and R. L. Phillips, “Laser beam propagation through random media,” *Laser Beam Propagation Through Random Media: Second Edition*, 2005.

- [5] L. C. Andrews, R. L. Phillips, R. J. Sasiela, and R. R. Parenti, “Strehl ratio and scintillation theory for uplink gaussian-beam waves: beam wander effects,” *Optical Engineering*, vol. 45, no. 7, pp. 076001–076001, 2006.
- [6] A. K. Majumdar and J. C. Ricklin, *Free-space laser communications: principles and advances*. Springer Science & Business Media, 2010, vol. 2.
- [7] H. Hemmati, *Near-earth laser communications*. CRC press, 2020, vol. 1.
- [8] S. Zhao, B. Luo, A. Dang, and H. Guo, “Optimum transmitter radius for ground-to-satellite laser uplink communication systems in the presence of beam wander effect,” in *Applications of Lasers for Sensing and Free Space Communications*. Optica Publishing Group, 2010, p. LSMD2.
- [9] S. L. Odintsov, V. A. Gladkikh, A. P. Kamardin, and I. V. Nevzorova, “Determination of the structural characteristic of the refractive index of optical waves in the atmospheric boundary layer with remote acoustic sounding facilities,” *Atmosphere*, vol. 10, no. 11, p. 711, 2019.
- [10] S. Fiorino, S. Bose-Pillai, and K. Keefer, “Re-visiting acoustic sounding to advance the measurement of optical turbulence,” *Applied Sciences*, vol. 11, no. 16, p. 7658, 2021.
- [11] D. Jian, S. Teng-fei, and L. Yu, “A review of daytime atmospheric optical turbulence profile detection technology,” *Chinese Astronomy and Astrophysics*, vol. 47, no. 2, pp. 257–284, 2023.
- [12] A. Puryear, R. Jin, E. Lee, and V. W. Chan, “Experimental analysis of the time dynamics of coherent communication through turbulence: Markovianity and channel prediction,” in *2011 International Conference on Space Optical Systems and Applications (ICSOS)*. IEEE, 2011, pp. 28–37.
- [13] M. A. Kashani, M. Uysal, and M. Kavehrad, “A novel statistical channel model for turbulence-induced fading in free-space optical systems,” *Journal of Lightwave Technology*, vol. 33, no. 11, pp. 2303–2312, 2015.
- [14] A. Lionis, G. Chaskakis, K. Cohn, J. Blau, K. Peppas, H. E. Nistazakis, and A. Tsigopoulos, “Optical turbulence measurements and modeling over monterey bay,” *Optics Communications*, vol. 520, p. 128508, 2022.
- [15] F. Quatresooz, G. O. de Xivry, O. Absil, D. Vanhoenacker-Janvier, and C. Oestges, “Challenges for optical turbulence characterization and prediction at optical communication sites,” in *International Conference on Space Optics—ICSO 2022*, vol. 12777. SPIE, 2023, pp. 2410–2424.
- [16] A. Lionis, A. Sklavounos, A. Stassinakis, K. Cohn, A. Tsigopoulos, K. Peppas, K. Aidinis, and H. Nistazakis, “Experimental machine learning approach for optical turbulence and FSO outage performance modeling,” *Electronics*, vol. 12, no. 3, p. 506, 2023.
- [17] S. Lohani and R. T. Glasser, “Turbulence correction with artificial neural networks,” *Optics letters*, vol. 43, no. 11, pp. 2611–2614, 2018.
- [18] M. A. Esmail, W. S. Saif, A. M. Ragheb, and S. A. Alshebeili, “Free space optic channel monitoring using machine learning,” *Optics Express*, vol. 29, no. 7, pp. 10967–10981, 2021.
- [19] M8195A 65 GSa/s Arbitrary Waveform Generator. Keysight. Accessed on: 3-2-2024. [Online]. Available: <https://www.keysight.com/us/en/product/M8195A/65-gsa-s-arbitrary-waveform-generator.html>
- [20] DSOV254A Infiniium V-Series Oscilloscope: 25 GHz, 4 Analog Channels. Keysight. Accessed on: 3-2-2024. [Online]. Available: <https://www.keysight.com/us/en/product/DSOV254A/infiniium-v-series-oscilloscope-25-ghz-4-analog-channels.html>
- [21] O. Sagi and L. Rokach, “Ensemble learning: A survey,” *Wiley Interdisciplinary Reviews: Data Mining and Knowledge Discovery*, vol. 8, no. 4, p. e1249, 2018.
- [22] S. Fatima, A. Hussain, S. B. Amir, S. H. Ahmed, and S. M. H. Aslam, “Xgboost and random forest algorithms: An in depth analysis,” *Pakistan Journal of Scientific Research*, vol. 3, no. 1, pp. 26–31, 2023.
- [23] D. Brain and G. I. Webb, “On the effect of data set size on bias and variance in classification learning,” in *Proceedings of the Fourth Australian Knowledge Acquisition Workshop, University of New South Wales*, 1999, pp. 117–128.